# Inductive Coupled In-Circuit Impedance Monitoring of Electrical System Using Two-Port *ABCD* Network Approach

Kang Rong Li, Kye Yak See, *Senior Member, IEEE*, and Xing Ming Li

***Abstract*— By treating the inductive coupling probes and the electrical system to be monitored as three cascaded two-port *ABCD* networks, the in-circuit impedance of the electrical system can be extracted with ease. The proposed method simplifies the setup calibration and allows real-time impedance monitoring of critical electrical system to be implemented without interrupting its normal operating conditions. In this paper, the theory behind the proposed *ABCD* networks approach is described. The proposed approach has overcome the poor measurement accuracy of the conventional inductive coupling calibration method above 30 MHz and has achieved good accuracy up to 100 MHz with a maximum measurement deviation of 3.6%. Finally, using a dc-powered motor as a practical example, the ability to detect the change of in-circuit impedance of the motor under different operating conditions is demonstrated.**

***Index Terms*— In-circuit impedance monitoring, inductive coupling, two-port *ABCD* parameters.**

## I. Introduction

THE ability to extract in-circuit impedance of a critical electrical system is important for condition monitoring purposes. Most of the methods for in-circuit impedance measurement are usually intended for very specific applications [1]–[3]. More general in-circuit impedance measurement methods have also been developed based on the inductive coupling technique [4]–[6]. The inductive coupling method which uses two clamp-on type current probes, one as injecting probe and another as receiving probe, has been applied to extract in-circuit noise source impedance for the purposes of electromagnetic interference filter design [7]–[9] and impedance characterization of in-circuit ferrite-core inductor [10]. A current probe clamped onto a cable is basically an inductive coupling transformer with a turn ratio of $N$:1, where the side with $N$ turns connects to the signal source (injecting) or the measuring instrument (receiving); and the side with one turn refers to the cable being clamped. The attractive feature of using current probes for in-circuit impedance measurement is that the probes do not have direct electrical contact to the system being measured, and hence, can be easily mounted on-site for any high-voltage electrical system under its normal condition without safety hazard concern.

However, the inductive coupling method requires laborious premeasurement calibration. It is first done with a known standard precision resistor as a device under test (DUT), and then it is repeated again with the DUT replaced with a short circuit as described in detail in Section II. For many practical applications, the DUT cannot be easily replaced with a known standard resistor due to either its size or inaccessibility. In addition, the calibration under short-circuit condition can only be carried out when the system is cutoff from the power supply, which may not be always feasible if the system is mission critical. In addition, the method requires the calibration be repeated for every different circuit or system to be measured. Hence, the method cannot be easily applied for practical real-time impedance monitoring purposes. In addition, the accuracy of the inductive coupling method is found to be influenced by the value of the standard precision resistor selected for the premeasurement calibration, which will be elaborated in Section IV.

To address these practical issues of the inductive coupling method, this paper proposes an *ABCD* two-port network approach for the extraction of in-circuit impedance of any electrical system. The *ABCD* two-port network also known as chain parameters, allows cascading of two or more networks by simply multiplying the characterized matrices of the instruments used in the measurement setup. The electrical system to be monitored and the current probes used can be characterized individually, and then cascaded using the *ABCD* parameters with ease.

This paper is organized as follows. It briefly describes the existing inductive coupling method and its constraints. Then, it proposes the in-circuit impedance extraction based on the concept of *ABCD* two-port network and validates the proposed approach experimentally. Finally, a practical example is shown to demonstrate how the proposed approach can be deployed for condition monitoring through in-circuit impedance extraction.

## II. Review of the Inductive Coupling Method

The basic measurement setup of the inductive coupling method is shown in Fig. 1. The instruments for the setup consist of an injecting current probe, a receiving current probe, and a vector network analyzer (VNA). An RF signal

Manuscript received August 9, 2014; revised December 9, 2014; accepted December 15, 2014. The Associate Editor coordinating the review process was Dr. Wendy Van Moer.

K. R. Li and K. Y. See are with the Nanyang Technological University, Singapore 639798 (e-mail: kli2@e.ntu.edu.sg).

X. M. Li is with the Beijing Institute of Technology, Beijing 100081, China.

Color versions of one or more of the figures in this paper are available online at http://ieeexplore.ieee.org.

Digital Object Identifier 10.1109/TIM.2015.2403091

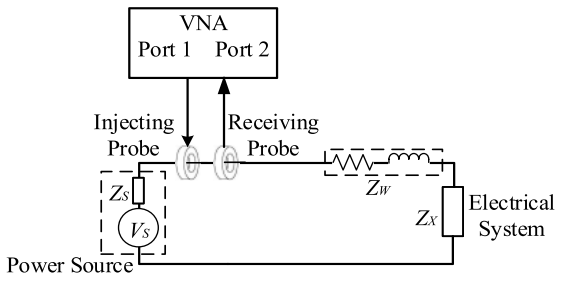


Fig. 1. Basic measurement setup of the inductively coupling method.

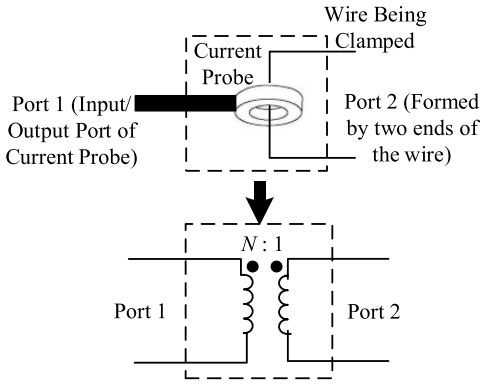


Fig. 2. Equivalent two-port network formed by the current probe and wire.

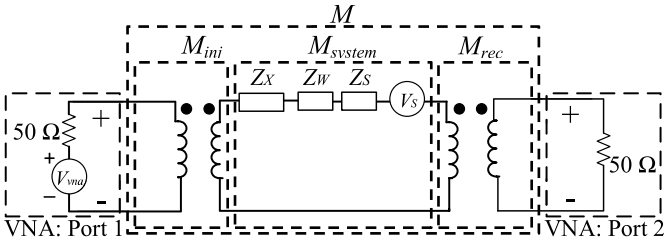


Fig. 3. Equivalent two-port network of the measurement setup in Fig. 1 with three cascaded two-port networks $M_{\text{inj}}$, $M_{\text{system}}$, and $M_{\text{rec}}$.

is injected to the circuit loop, which consists of the electrical system, the power source, and the wiring connection to the electrical system and the power source, from VNA's port 1 through the injecting probe and the same signal is received at VNA's port 2 through the receiving probe. The electrical system is powered by a power source, $V_S$, which can be either a dc of ac power source. $Z_S$ is the power source impedance. $Z_X$ is the impedance of the electrical system under its power-up condition. $Z_W$ is equivalent series resistance and series inductance of the wiring connection. The resultant in-circuit impedance $Z_{\text{system}}$ of the electrical system being monitored is the sum of $Z_X$, $Z_S$, and $Z_W$. Usually, $Z_{\text{system}}$ is dominated by $Z_X$, as $Z_S$ and $Z_W$ are relatively small.

The measurement setup must be carefully calibrated with the power source disconnected. First, one set of $S$-parameters is measured with $Z_X$ replaced by a known standard precision resistor. Then, another set of $S$-parameters is measured again with $Z_X$ replaced by a short circuit. Finally, one more set of $S$-parameters is measured with the power source connected to the electrical system, as shown in Fig. 1, using the same VNA with the electrical system powered up. With the three sets of $S$-parameters, $Z_{\text{system}}$ can be estimated [7].

## III. In-Circuit Impedance Extraction Using Two-Port *ABCD* Network

As mentioned in the earlier section, the premeasurement calibration of the inductive coupling method requires the power source to be disconnected, so that the electrical system can be replaced with a known resistor and a short circuit. However, in reality, cutting the power off from an electrical system may not always be feasible due to the criticality of the system. Even cutting off the power is feasible; the electrical system may not be easily assessable for the replacement of standard resistor or short circuit. To overcome these constraints, an alternative approach to extract the in-circuit impedance is proposed.

The current probe and the wire being clamped is basically a transformer with turn ratio of $N$:1 [8]–[10], as shown in Fig. 2. The transformer can be represented as a two-port network where one port is the input (or output) port of the current probe and the other port is the two ends of the wire being clamped. Hence, the injecting probe, the receiving probe, and the electrical system being monitored, as shown in Fig. 1, can be modeled as three cascaded two-port networks, as shown in Fig. 3.

$M_{\text{inj}}$ is the two-port inductive coupling network of the injecting probe with the wire being clamped. $M_{\text{system}}$ represents the two-port network consisting of the electrical system, the power source, and the wiring connection. $M_{\text{rec}}$ is the two-port inductive coupling network of the receiving probe with the wire being clamped. $V_{\text{vna}}$ is the signal source at port 1 of the VNA. With the network representation in Fig. 3, the two-port network $M$ between ports 1 and 2 is related by

$$\begin{bmatrix} A & B \\ C & D \end{bmatrix} = \begin{bmatrix} A & B \\ C & D \end{bmatrix}_{\text{inj}} \begin{bmatrix} A & B \\ C & D \end{bmatrix}_{\text{system}} \begin{bmatrix} A & B \\ C & D \end{bmatrix}_{\text{rec}} \quad (1)$$

where $\begin{bmatrix} A & B \\ C & D \end{bmatrix}$ $\begin{bmatrix} A & B \\ C & D \end{bmatrix}_{\text{inj}}$, $\begin{bmatrix} A & B \\ C & D \end{bmatrix}_{\text{system}}$, and $\begin{bmatrix} A & B \\ C & D \end{bmatrix}_{\text{rec}}$ are the *ABCD* parameters of $M$, $M_{\text{inj}}$, $M_{\text{system}}$, and $M_{\text{rec}}$, respectively.

By solving $M_{\text{system}}$, one can obtain $Z_{\text{system}}$ under its in-circuit condition since the parameter $B$ of $M_{\text{system}}$ equals to $Z_{\text{system}}$ [11]. From (1), $M_{\text{system}}$ can be solved once $M$, $M_{\text{inj}}$, and $M_{\text{rec}}$ are obtained. Before the actual in-circuit impedance measurement, $M_{\text{inj}}$ and $M_{\text{rec}}$ must be first characterized using the test fixture, as shown in Fig. 4.

The fabricated test fixture, which is designed to characterize two Tektronix CT1 current probes (25 KHz to 1 GHz) [12] as injecting and receiving probes for the in-circuit measurement, is a single layer double-sided Printed Circuit Board (PCB) (1.5-mm thickness) with a full ground plane on the bottom side. The CT1 with a hole diameter of AWG 14 is clamped onto an AWG 22 wire of 3-cm length, which is the shortest possible length to minimize the impact of the parasitic effect of the wire in the characterized *ABCD* parameters.

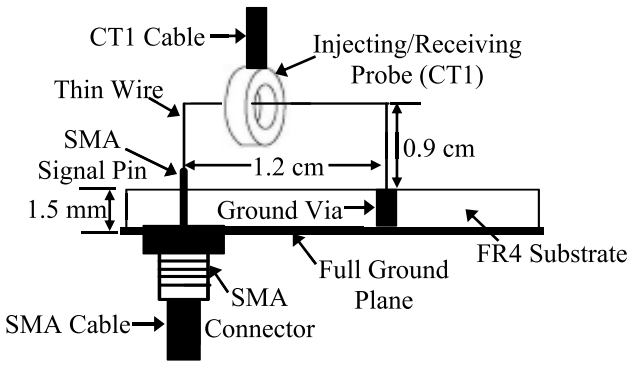


Fig. 4. Test fixture to characterize injecting and receiving probes (side view).

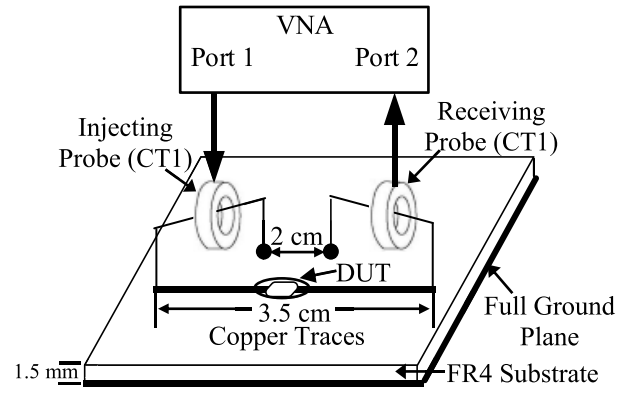


Fig. 5. Setup and the Printed Circuit Board for experimental validation (3-D view).

One end of the wire is connected to the signal pin of the SubMiniature version A (SMA) connector and the other end connected to the ground plane through a via. The SMA connector is to facilitate the connection to the R&S ZVB8 VNA (300 KHz to 8 GHz), which is also employed for the subsequent measurements.

To characterize $M_{\text{inj}}$, ports 1 and 2 of the VNA are connected to the injecting probe and SMA connector, respectively. To characterize $M_{\text{rec}}$, ports 1 and 2 of the VNA are connected to SMA connector and the receiving probe, respectively. Once $M_{\text{inj}}$ and $M_{\text{rec}}$ are characterized, $M$ is measured by clamping the two current probes onto the wire between the electrical system and the power source.

With $M$, $M_{\text{inj}}$, and $M_{\text{rec}}$ characterized, $M_{\text{system}}$ can be solved easily.

$M_{\text{inj}}$ and $M_{\text{rec}}$ are reusable as long as the same probes are employed in the measurements, and hence, only $M$ needs to be remeasured for different electrical systems.

## IV. Experimental Validation and Accuracy

### A. Validation

For validation purpose, two CT1 probes precharacterized with the test fixture shown in Fig. 4 are employed as the injecting and the receiving current probes connecting to ports 1 and 2 of the VNA, respectively.

Fig. 5 shows the setup on PCB for experimental validation. The PCB (1.5-mm thickness) has two sections of copper traces (total length of 3.5 cm and width of 0.2 cm) connecting two ends of two AWG 22 wires (each 3 cm in length) on the upper side of the PCB. Two vias on the PCB with a separation distance of 2 cm connect the other two ends of the wires to the ground plane on the lower side of the PCB. Passive components with known values are treated as unknown DUT placed between the two copper traces. The components are Surface Mounted Devices (SMD) resistors: 30 Ω, 51 Ω, 62 Ω, 110 Ω, 150 Ω, 510 Ω, and 1 kΩ; SMD capacitors: 4.7 and 6.8 pF; and axial-lead ferrite-core inductors: 4.7 and 47 $\mu$H. The circuit loop consisting of the wires, copper traces, and ground plane is electrically small as compared with the wavelength of 100 MHz the highest frequency for the measurement.

The injecting and receiving CT1 probes clamped onto the wires form $M_{\text{inj}}$ and $M_{\text{rec}}$, respectively. The DUT and the wiring connection 1 probes clamped onto the wires form $M_i$ to the DUT form $M_{\text{system}}$. Therefore, the in-circuit impedance to be measured will be the DUT impedance and wiring impedance in series. The impedance incurred by the wiring connection is found to be far smaller than the DUT impedance throughout the frequency range up to 100 MHz. Thus, the measured impedance is dominated by the DUT impedance.

The impedance of each of these passive components is measured separately with an impedance analyzer. The measured impedance using the proposed approach is compared with the measured impedance using the impedance analyzer and plotted in Figs. 6 and 7. The measured impedance of the wiring connection is plotted in Fig. 8.

As shown in Figs. 6 and 7, the measured impedance from the proposed method (dotted lines) are in close agreement with measured impedance from an impedance analyzer (dashed lines) up to 100 MHz. Fig. 8 shows that the measured impedance of the wiring connection, which is inductive in nature, is very small and less than 2.6 Ω at the highest frequency of 100 MHz.

The measurement results have demonstrated that the proposed method has the ability to measure in-circuit impedance up to 100 MHz with good accuracy. The maximum frequency of the in-circuit measurement depends very much on the effective bandwidth of the current probes. Although the CT1's user manual specifies its transfer impedance $Z_T$ is 5 Ω with a bandwidth from 25 KHz to 1 GHz, the actual effective bandwidth is found to be 1–100 MHz [12]. It is noted that the stated $Z_T$ is calibrated with a 50-Ω load in the circuit loop when it is configured as a receiving probe [13]. In reality, the frequency response of $Z_T$ can vary with the load impedance in the circuit loop. According to the measurement setup in [13], the aforementioned test fixture with the same wire for characterization, the VNA, SMD resistors (10 Ω, 51 Ω, 150 Ω, and 1 kΩ), and a CT1 probe as a receiving probe are used to observe the variation of $Z_T$ of CT1. The test setup for is shown in Fig. 9.

In Fig. 9, the SMD resistor is soldered on the fixture, where there are two short sections of copper traces connecting both ends of the SMD resistor to the SMA connector's signal pin and the ground plane of the text fixture, respectively. The SMA connector and the CT1 current probe are connected to ports 1 and 2 of the VNA, respectively. The CT1 probe clamped onto the wire receives the RF signal injected from VNA's port 1.

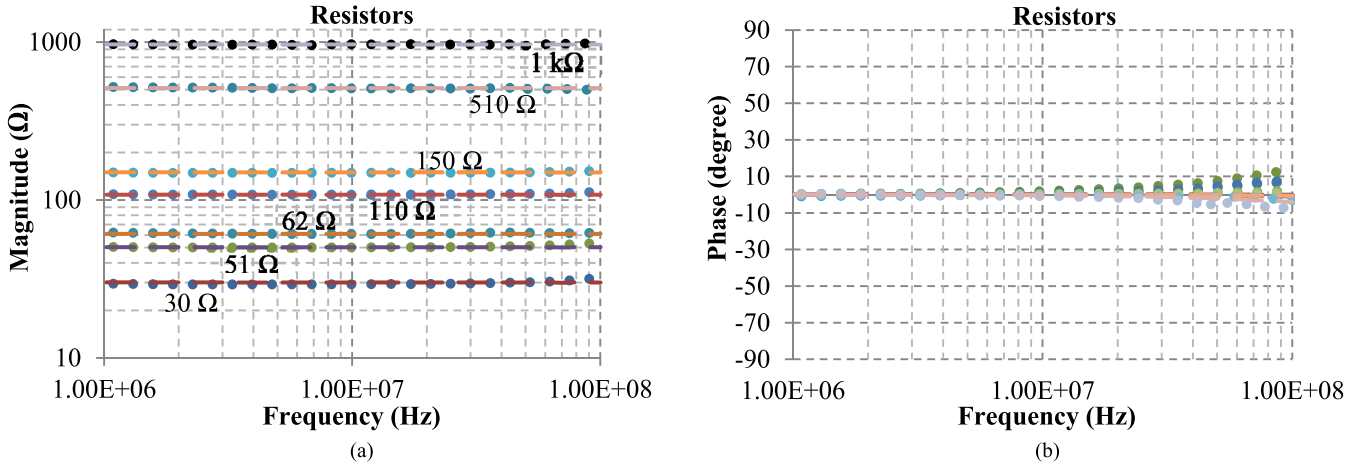


Fig. 6. Impedances of resistors measured with the proposed approach (dotted lines) and with impedance analyzer (dashed lines). (a) Magnitudes. (b) Phases.

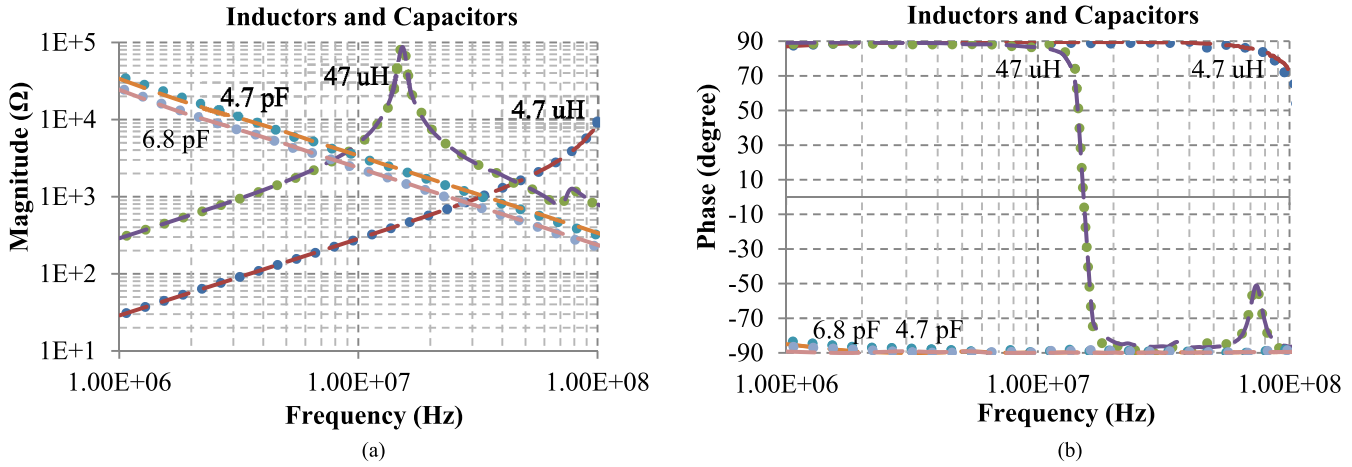


Fig. 7. Impedances of inductors and capacitors measured with the proposed approach (dotted lines) and with impedance analyzer (dashed lines). (a) Magnitudes. (b) Phases.

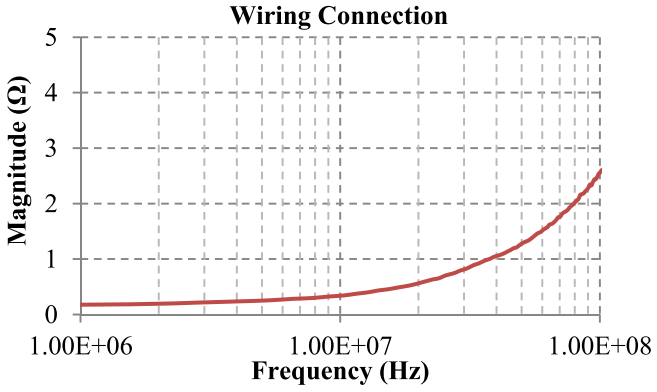


Fig. 8. Impedance magnitude of the wiring connection measured with the proposed approach.

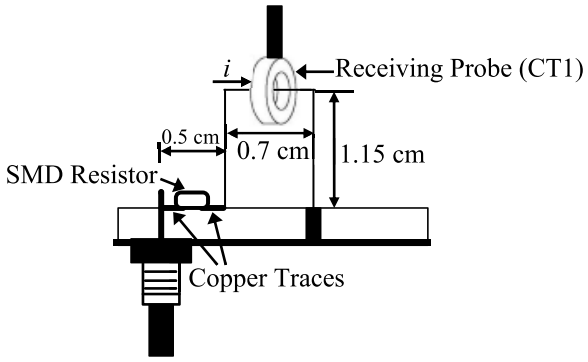


Fig. 9. Setup to measure $Z_T$ of CT1on the test fixture (side view).

$Z_T$ of CT1 can be computed from

$$Z_T = \frac{V_2^-}{i} \tag{2}$$

where $V_2^-$ is the received voltage measured at port 2 through CT1 and $i$ is the current due to the injected signal from port 1, which is given by

$$i = \frac{V_1}{Z_R} = \frac{V_1^+(1+S_{11})}{Z_R} \tag{3}$$

where $V_1$ is the voltage across the SMD resistor and $V_1^+$ is the signal source voltage of port 1. $Z_R$ is the impedance of

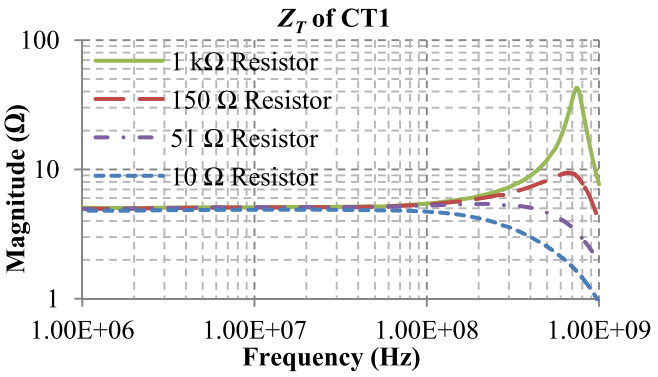


Fig. 10. Magnitude of CT1's $Z_T$ with different resistors on the test fixture.

TABLE I
COMPARISON BETWEEN TWO APPROACHES

| Frequency (MHz) | Deviation of Conventional Approach (%) | | Deviation of Proposed Approach (%) |
|---|---|---|---|
| | Setup Calibration with $R_{std}$=30 Ω | Setup Calibration with $R_{std}$=1 kΩ | |
| 1 | + 1.4 | + 2.2 | + 0.3 |
| 10 | + 1.9 | + 2.2 | + 0.1 |
| 30 | + 1.5 | + 3.6 | + 0.6 |
| 50 | − 0.5 | + 5.8 | + 0.7 |
| 70 | − 2.7 | + 9.8 | + 1.1 |
| 100 | − 8.5 | + 15.5 | + 3.6 |

the SMD resistor. Substituting (3) into (2) leads to

$$Z_T = \frac{Z_R \cdot V_2^-}{V_1^+ \cdot (1 + S_{11})} = \frac{Z_R \cdot S_{21}}{1 + S_{11}}. \quad (4)$$

Thus, four frequency response curves of $Z_T$ under different resistive loads are plotted up to 1 GHz and shown in Fig. 10.

As shown in Fig. 10, $Z_T$ for all four resistive loads remains constant at 5 Ω but begins to deviate above 100 MHz. It shows that the effective bandwidth of the probe is 100 MHz, where $Z_T$ is insensitive to the large variation of the impedance to be measured. Thus, we are confident that the results from the proposed method using CT1 probes are of good accuracy up to 100 MHz.

### *B. Accuracy Comparison*

As mentioned earlier, the measurement accuracy of existing inductive coupling method [7]–[10] is sensitive to the value of the precision resistor chosen for the setup calibration. To illustrate this issue, a 110-Ω SMD resistor is used as a DUT. It is first measured with the existing method when two different precision resistors ($R_{\text{std}}$ = 30 Ω and 1 kΩ) are chosen for the setup calibration. Then, it is remeasured again with the proposed approach described in this paper. The measurement results are plotted in Fig. 11 for comparison with the measured impedance using an impedance analyzer as a reference. For ease of comparison, the deviations of the measured impedances from the two approaches from the impedance analyzer result are tabulated in Table I.

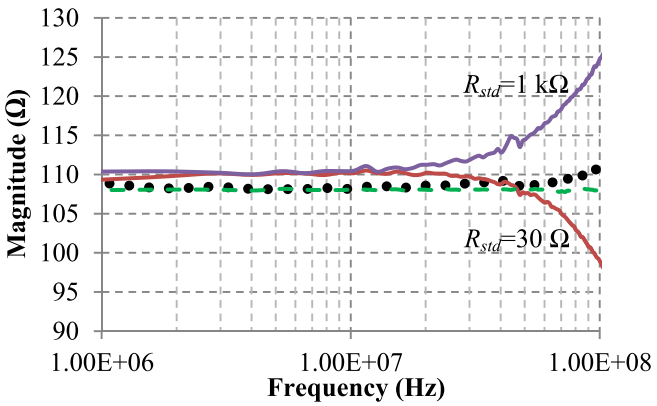


Fig. 11. Measured impedance of the 110-Ω SMD resistor with existing method (solid lines), proposed method (dotted line), and impedance analyzer (dashed line).

Fig. 11 shows that measured impedance with the proposed method (dotted line) is in close agreement with that measured with impedance analyzer (dashed line) across the frequency range up to 100 MHz. However, the measured impedance using the existing method (solid lines) with different calibration precision resistors (30 Ω and 1 kΩ) starts to deviate at when the frequency exceeds 30 MHz and deviation becomes significant with increasing frequency. Table I shows that the deviation of the existing approach at 100 MHz can be as high as −8.5% if 30 Ω is used for the setup calibration or +15.5% if 1 kΩ is chosen for the setup calibration. The worst deviation of the proposed approach is only +3.6% at 100 MHz. The results reveal that for the existing approach can only achieve good measurement accuracy at higher frequencies if the calibration resistor is as close to the impedance of the DUT as possible. Unfortunately, this prior knowledge may not be readily available in reality. On the other hand, the proposed approach overcomes this constraint and becomes attractive for accurate in-circuit impedance monitoring in many practical applications.

## V. IN-CIRCUIT IMPEDANCE MEASUREMENT FOR CONDITION MONITORING

To illustrate how the proposed method can be applied for in-circuit impedance monitoring purposes, an FA-130 dc motor powered by a Caltron PR-3504D dc-power supply is used as an example. The source voltage is kept at 3 V and the proposed inductive coupling method is employed to measure the in-circuit impedance under two different operating conditions. For the first operating condition, there is no object attached to the motor's axle (denoted as unloaded condition). For the second operating condition, an object weighed 6 g is attached to the motor axle (denoted as loaded condition). For the unloaded condition, the motor spins at higher speed and for the loaded condition, the motor spins at lower speed. The measurement setup is shown in Fig. 12.

As shown in Fig. 12, two AWG 22 wires, each 4 cm in length, connect the motor to the power supply. An RF signal is induced to the electrical system that consists of the power supply, the connecting wires, and the motor, through

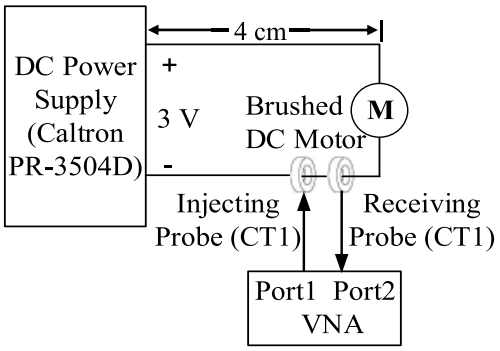


Fig. 12. In-circuit measurement setup on the operating dc motor.

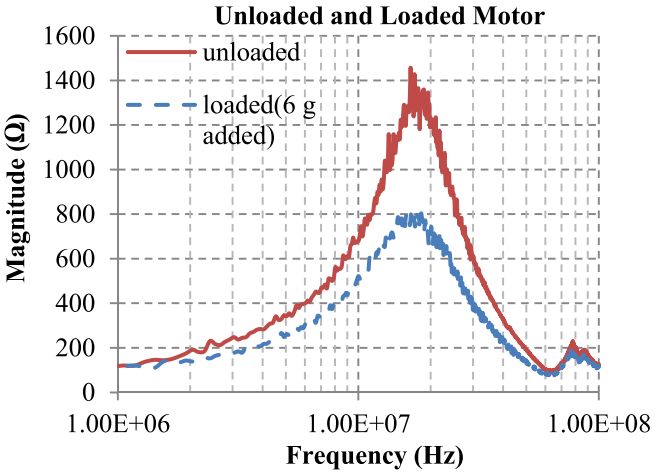


Fig. 13. In-circuit impedances of the operating motor system under unloaded and loaded conditions.

an injecting CT1 probe. The RF signal is picked up by the receiving CT1 probe.

As mentioned in Section III, since the *ABCD* parameters of the two CT1 probes have been precharacterized, only two more measurements are needed to extract the in-circuit impedances of the powered up motor system under unloaded and loaded conditions. The in-circuit impedances are extracted and shown in Fig. 13.

Fig. 13 shows that the impedance is inductive in nature, as it is dominated by the motor's coil winding. The parasitic capacitance of the coil causes a resonant frequency at around 16 MHz, and above 16 MHz, the impedance is dominated by the parasitic capacitance. The impedance under unloaded condition is noticeably higher than that under the loaded condition. Based on the impedance response below the resonant frequency, the inductances of the motor coil under unloaded and loaded conditions are 11 and 8 $\mu$H, respectively.

The drop in coil inductance is expected due to the saturation of the soft iron core, where the coil windings are wound. The dc supply current to the motor increases from 0.65 to 1.80 A when the 6-g load is applied to the motor. The increase in dc current to the motor has resulted in core saturation. Through this example, it has demonstrated that the proposed method has the ability to monitor the impedance change of an electrical system under different operating conditions. The ability to monitor the change is useful so that any unusual behavior of the system can be detected early and rectified.

## VI. Conclusion

Based on a two-port *ABCD* network approach, this paper proposes a method to extract in-circuit impedance of any electrical system accurately under its operating conditions. Using a precision 110-Ω SMD resistor as a DUT, the proposed method has demonstrated its measurement accuracy up to 100 MHz with a maximum deviation of 3.6%. As opposed to the existing inductive coupling method, the proposed method eliminates the need of a standard precision resistor for its setup calibration, and therefore its measurement accuracy is independent of the setup resistor value. The in-circuit measurement of a dc motor under its usual operation has also demonstrated that the proposed method can detect the change of the in-circuit impedance for real-time condition monitoring purpose. The proposed method also does not require the power supply to the system to be disconnected for setup calibration. The injecting and receiving probes used need only one-time characterization to obtain the *ABCD* parameters and are reusable for subsequent measurements. Although the example shown is a dc motor operated at low-voltage dc, the proposed method can be extended to high-voltage electrical system, of course with a larger current probe and bigger wire size for precharacterization. The proposed method opens the doors for real-time condition monitoring of high-voltage electrical system for detection of early signs of potential faults before the system breaks down.

## References

[1] J.-W. Tan, R.-J. Liao, H. Wang, L. Li, and S.-Z. Qiang, "Time domain electrical impedance measurement method for ultrasound transducer," in *Proc. Int. Symp. Bioelectron. Bioinformat. (ISBB)*, Nov. 2011, pp. 279–282.

[2] G. Juping, J. Long, Q. Shenbei, W. Xinjian, and X. Zhike, "Researching on the automatic impedance measurement system," in *Proc. 8th Int. Conf. Elect. Mach. Syst. (ICEMS)*, vol. 3. Sep. 2005, pp. 2478–2481.

[3] J. Hoja and G. Lentka, "New measurement probe for high impedance spectroscopy," in *Proc. IEEE Instrum. Meas. Technol. Conf. (IMTC)*, Apr. 2006, pp. 323–328.

[4] M. Rahman, T. M. Ahmed, and V. Murti, "A TRA bridge technique for in-circuit impedance measurement," *IEEE Trans. Instrum. Meas.*, vol. 33, no. 4, pp. 252–256, Dec. 1984.

[5] R. L. Forgacs, "In-circuit impedance measurement using current sensing," *IEEE Trans. Instrum. Meas.*, vol. IM-34, no. 1, pp. 6–14, Mar. 1985.

[6] R. A. Southwick and W. C. Dolle, "Line impedance measuring instrumentation utilizing current probe coupling," *IEEE Trans. Electromagn. Compat.*, vol. EMC-13, no. 4, pp. 31–36, Nov. 1971.

[7] V. Tarateeraseth, B. Hu, K. Y. See, and F. G. Canavero, "Accurate extraction of noise source impedance of an SMPS under operating conditions," *IEEE Trans. Power Electron.*, vol. 25, no. 1, pp. 111–117, Jan. 2010.

[8] K. Y. See and J. Deng, "Measurement of noise source impedance of SMPS using a two probes approach," *IEEE Trans. Power Electron.*, vol. 19, no. 3, pp. 862–868, May 2004.

[9] J. A. Malack and J. R. Engstrom, "RF impedance of United States and European power lines," *IEEE Trans. Electromagn. Compat.*, vol. EMC-18, no. 1, pp. 36–38, Feb. 1976.

[10] B. Hu, V. Tarateeraseth, K. Y. See, and Y. Zhao, "Assessment of electromagnetic interference suppression performance of ferrite core loaded power cord," *IET Sci., Meas. Technol.*, vol. 4, no. 4, pp. 229–236, Jul. 2010.

[11] D. M. Pozar, *Microwave Engineering*, 2nd ed. New York, NY, USA: Wiley, 1998.

[12] *AC Current Probes CT1 · CT2 · CT6 Data Sheet*, Tektronix, Beaverton, OR, USA, 2014.

[13] H. Sekiguchi and T. Funaki, "Proposal for Measurement Method of Transfer Impedance of Current Probe," *IEEE Trans. Electromag. Compat.*, vol. 56, pp. 871–877, 2014.

**Kang Rong Li** received the B.Eng. degree from Xidian University, Xi'an, China, in 2007, and the M.Eng. degree from the University of South Carolina, Columbia, SC, USA, in 2011. He is currently pursuing the Ph.D. degree with Nanyang Technological University, Singapore.

He was the Hardware Engineer with Gionee Communication Equipment Company, Ltd., Shenzhen, China, from 2007 to 2008. His current research interests include electromagnetic compatibility/electromagnetic interference measurement, signal integrity, and in-circuit impedance extraction.

**Kye Yak See** (SM'02) received the B.Eng. degree from the National University of Singapore, Singapore, in 1986, and the Ph.D degree from Imperial College London, London, U.K., in 1997.

He joined Nanyang Technological University (NTU), Singapore, as a Faculty Member. He was with Singapore Technologies Electronics, Singapore, as a Senior Engineer, from 1986 and 1991. From 1991 to 1994, he was a lead Design Engineer with ASTEC Custom Power, Singapore. He is currently an Associate Professor with the School of Electrical and Electronic Engineering, NTU. He holds a concurrent appointment as the Director of the Electromagnetic Effects Research Laboratory. His current research interests include electromagnetic interference filter, signal integrity, and electromagnetic compatibility measurement and design.

Dr. See was the Founding Chair of the IEEE Electromagnetic Compatibility (EMC) Chapter, and is the Chair of the IEEE Aerospace and Electronic Systems and the IEEE Geoscience and Remote Sensing Joint Chapter in Singapore. He was the Organizing Committee Chair of the EMC Zurich Symposium in 2006 and the Asia Pacific EMC Conference in Singapore in 2008. Since 2012, he has been the Technical Editor of the *IEEE Electromagnetic Compatibility Magazine*.

**Xing Ming Li** received the B.S. degree from the Beijing Institute of Technology, Beijing, China, in 2009, where he is currently pursuing the Ph.D. degree.

He was with the School of Electrical and Electronic Engineering, Nanyang Technological University, Singapore, as a Visiting Ph.D. Student, from 2012 to 2014. His current research interests include signal integrity and power integrity of high-speed systems, embedded system design for high-speed and real-time signal processing, and electromagnetic compatibility.